Journal of Power Sources 247 (2014) 84–89

Contents lists available at ScienceDirect

Journal of Power Sources

journal homepage: www.elsevier.com/locate/jpowsour

Effect of pre-oxidation on the oxidation resistance of spinel-coated Fe–Cr ferritic alloy for solid oxide fuel cell applications

Ding Rong Ou*, Mojie Cheng

Division of Fuel Cells and Battery, Dalian National Laboratory for Clean Energy, Dalian Institute of Chemical Physics, Chinese Academy of Sciences, 457 Zhongshan Road, Dalian 116023, China

HIGHLIGHTS

- Control of coating-alloy interface is important to SOFC metallic interconnects.
- Pre-oxidation treatment could improve oxidation resistance of spinel-coated SUS430.
- Reaction layer formed between the spinel coating and pre-oxidized alloy is a key.
- Dense $(Mn,Co,Cr)_3O_4$ reaction layer suppresses migrations of oxygen and chromium.
- With overall performance considered, an optimum thickness of reaction layer exists.

ARTICLE INFO

Article history:
Received 19 April 2013
Received in revised form
26 July 2013
Accepted 19 August 2013
Available online 31 August 2013

Keywords:
Solid oxide fuel cells
Metallic interconnects
High-temperature oxidation
Pre-oxidation
Interfacial reactions

ABSTRACT

Low-temperature-sintered $MnCo_2O_4$–MnO_2 coatings have been prepared on pre-oxidized SUS430 ferritic alloy by slurry coating. The effect of pre-oxidation treatment before slurry coating is then investigated. Microstructural and electrical characterizations show that 25 h of pre-oxidation at 800 °C could significantly improve the oxidation resistance of the coated alloy and effectively inhibit the increase in area-specific electrical resistance during long-term oxidation. These effects can be explained by the interfacial reactions between the coating and the pre-oxidized alloy during sintering and oxidation tests. Furthermore, this study suggests that the dense reaction layer at the coating-alloy interface could be the key to improving the oxidation resistance of metallic interconnects with low-temperature-sintered spinel coatings.

1. Introduction

The solid oxide fuel cell (SOFC) is a developing technology that can convert chemical energy into electrical energy with low emission and high energy conversion efficiency (≈60%). In recent years, due to the reduction of operating temperatures to below 850 °C, Fe–Cr ferritic alloys, e.g., type 430 alloy, ZMG 232 L and Crofer22 APU alloys, have been studied as interconnect materials for SOFCs [1–8]. Because they are less expensive than ceramic interconnects and exhibit good workability, metallic interconnects could greatly reduce the cost of SOFCs. However, the high-temperature oxidation of Fe–Cr ferritic alloys increases the area-specific electrical resistance (ASR) of metallic interconnects during long-term operation. Furthermore, the migration of chromium species through evaporation and/or solid-state diffusion may poison the cathode. To suppress the negative effects of metallic interconnects, a protective coating is usually applied to the alloy surface.

A promising coating material for Fe–Cr ferritic alloys is Mn–Co spinel oxide, which has a high electronic conductivity at the operating temperature of SOFCs and a thermal expansion coefficient (TEC) that matches that of ferric alloys [9–14]. In addition to the properties of coating materials, coating manufacturing processes are also important to the microstructural and electrical characteristics of coated metallic interconnects. To date, the most common method for preparing a spinel protective layer on metallic interconnects is slurry coating. However, green coatings of Mn–Co spinel oxides are difficult to densify at a temperature lower than 1000 °C [15]. To suppress the damage caused to metallic interconnects by high-temperature sintering, fundamental studies

* Corresponding author. Tel./fax: +86 411 84379028.
E-mail address: oudingrong@dicp.ac.cn (D.R. Ou).

0378-7753/$ – see front matter © 2013 Elsevier B.V. All rights reserved.
http://dx.doi.org/10.1016/j.jpowsour.2013.08.074

and technologically oriented studies have been conducted to reduce the sintering temperature of Mn–Co spinel coatings to a safe temperature for Fe–Cr ferritic alloys (i.e., ≤850 °C) [16–20]. For example, Yang et al. prepared $Mn_{1.5}Co_{1.5}O_4$ spinel coatings on Crofer22 APU alloy by reducing the coated samples at 800 °C for 24 h and then air-heating them at 800 °C [16]. Baba et al. also prepared $MnCo_2O_4$ spinel coatings on ZMG 232 L alloy by reducing the coated samples at 800 °C for 20 h and then air-heating them at 800–850 °C for 10–24 h [17]. On the other hand, Xin et al. reduced nanopowders of spinel oxides, prepared green coatings on Crofer22 APU alloy using the reduced powders and then heated the coated alloy to 800–900 °C in air for densification [18,19]. These studies suggest that, through the reduction of spinel coatings [16,17] or oxide powders [18,19], metallic cobalt and manganese oxides with lower valence states can form. Thus, the reduction products can be oxidized during the following air sintering process and facilitate the densification of the protective coatings. However, from a cost perspective, the reduction of oxide powders or green coating makes the coating preparation process more complicated and more expansive.

Recently, the authors suggested a simple but effective approach, multi-component materials design, to achieve the low-temperature fabrication of protective coatings for Fe–Cr ferritic alloys [20]. The previous study demonstrated that low-temperature-sintered $MnCo_2O_4$–MnO_2 coatings were stable during cyclic oxidation tests and effective in improving the oxidation resistance of SUS430 alloy. To increase the adhesion of the green coatings to the substrates, the alloy needed to be pre-oxidized at 800 °C before slurry coating. In the present study, it was shown that this pre-oxidation treatment is also critically important to the oxidation resistance of the coated alloy. Through microstructural and electrical characterizations of the coated samples submitted to different pre-oxidation treatments, the effect of pre-oxidation on the interfacial reactions and thereby the oxidation resistance were investigated.

2. Experimental

The ferritic alloy studied was SUS430, a commercial product of Shanxi Taiyuan Stainless Steel Co. Ltd., with a chemical composition of 16.36 wt% Cr, 0.24 wt% Mn, 0.37 wt% Si, 0.09 wt% Ni, 0.04 wt% C, 0.016 wt% P, 0.001 wt% S and balance Fe. The steel sheet, with a thickness of 2.0 mm, was cut into 20 mm × 20 mm rectangular plates and ground with SiC abrasive paper of #320–#1000. After polishing, the surfaces of the samples were cleaned in an ultrasonic ethanol bath.

$MnCo_2O_4$–MnO_2 bi-component coatings were prepared on SUS430 plates by slurry dipping as described in a previous study [20]. To enhance the adhesion of the green coating to the polished alloy surface, the plates were pre-oxidized at 800 °C for 2–100 h before coating the slurry. A slurry consisting of a mixture of $MnCo_2O_4$ and MnO_2 powders, PVB and ethanol was prepared and applied to the pre-oxidized plates by dip-coating. In the slurry, the mole ratio of MnO_2 to $MnCo_2O_4$ was set to 0.5:1, i.e., the average atomic ratio of Mn/Co in the mixture was designed to be 0.75. Then, the green coating was dried and sintered at 800 °C for 8–50 h.

Cyclic oxidation tests of coated SUS430 plates were performed in ambient air. In a test cycle, the plates were heated to 800 °C at 5 °C min^{-1}, held at that temperature for 50 h and then cooled to room temperature. The electrical resistance of plate samples was measured by a four-probe DC technique using Au electrodes. After the alloy was held at the measurement temperatures for 30–60 min for stabilization, the measurements were performed in air. The values of ASR (expressed in mΩ cm^2) of the oxide scales and protective coatings were calculated according to Ohm's law, ASR = $AU/2I$, where A is the sample area, U is the voltage drop and I is the electric current. A factor of 2 was included to account for the fact that the voltage drop was measured across two oxide scales or coatings connected in series. Then, the activation energy (E_a) for electric conduction was estimated using the following equation:

$$T/\mathrm{ASR} = k\exp(-E_a/RT), \quad (1)$$

where T is the measurement temperature and k is a constant that depends only on sample properties.

The crystal structures of the coatings were analyzed by X-ray diffraction (XRD) using a Rigaku D/Max2500VB2 X-ray Generator with Cu Kα radiation. The diffraction peaks were identified according to the lattice constants indicated by JCPDS cards [21]. Microstructural and compositional characterizations were performed using a FEI scanning electron microscope (SEM, model Quanta 200FEG) equipped with an energy-dispersive X-ray spectroscopy (EDX) instrument. After analyzing the surface, sample cross-sections were prepared by epoxy mounting and polishing and further examined by SEM and EDX.

3. Results and discussions

Fig. 1 shows the XRD profiles of $MnCo_2O_4$–MnO_2-coated samples pre-oxidized for 2 h and 25 h. After being held at 800 °C for 1000 h, the protective coatings on both samples were dominated by $(Mn,Co)_3O_4$ solid solutions. It has been suggested that the $(Mn,Co)_3O_4$ solid solutions are products of the solid-state reaction between MnO_2 and $MnCo_2O_4$, which could facilitate the densification of the protective coatings, and that the shifts of diffraction peaks belonging to spinel oxides could be due to the dissolution of Mn oxide into $MnCo_2O_4$ [20]. Furthermore, weak diffractions belonging to Cr_2O_3 can be seen on the profile of the sample pre-oxidized for only 2 h, demonstrating that oxidation of the metallic substrate might take place beneath the protective layer.

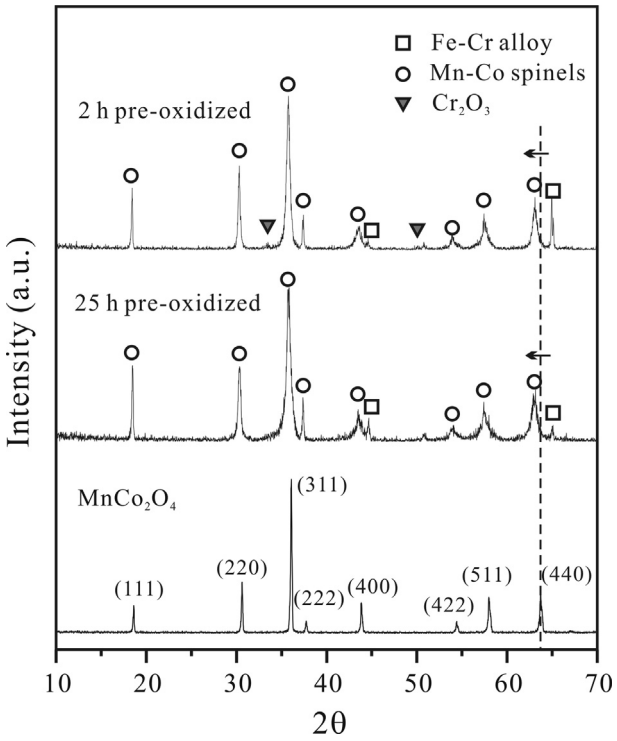

Fig. 1. XRD profiles of $MnCo_2O_4$–MnO_2-coated SUS430 plates after oxidation at 800 °C for 1000 h. The profile of $MnCo_2O_4$ powder is also presented for comparison.

To explore the microstructural features of the coated SUS430 plates submitted to different pre-oxidation treatments, SEM and EDX studies were performed. Fig. 2 shows the surface morphologies of the coated samples after being held at 800 °C for 1000 h in air. On the sample pre-oxidized for only 2 h, net-like shallow hollows or cracks can be readily seen in the coating. The distribution of these hollows or cracks implies that they might occur along the grain boundary of the metallic substrate and their formation could be attributed to the metal oxidation beneath the coating. In contrast, the protective coating on the sample pre-oxidized for 25 h is free of visible cracks.

The difference in the microstructural features between two samples can also be observed in cross-sectional images (Figs. 3 and 4). On the EDX line-scan profiles of both samples, a gradient change of elements at the coating-alloy interface can be observed (as indicated by gray windows in Figs. 3 and 4). In this layer, the contents of Mn and Co decrease from the coating side, whereas the Cr content decreases from the alloy/scale side. Because it simultaneously contains Mn, Co and Cr, this layer could be the product of solid-state reactions and diffusion between the pre-oxidized alloy and the $MnCo_2O_4$–MnO_2 coating. As shown in Figs. 3 and 4, the thickness of the reaction layer is approximately 1 μm in both samples. In addition to the reaction layer, a Cr-rich layer with a thickness of approximately 2 μm (marked by a slash texture) can be observed on the sample pre-oxidized for only 2 h, which is located between the alloy and the reaction layer (Fig. 3). According to the XRD profiles shown in Fig. 1, this Cr-rich layer could be Cr_2O_3 produced during long-term oxidation. However, no clear chromium oxide layer can be observed when the pre-oxidation time increases to 25 h (Fig. 4), indicating that the oxidation resistance of the sample pre-oxidized for 25 h is much better than that pre-oxidized for 2 h.

To clarify the specific reactions between chromium oxides and different components in the $MnCo_2O_4$–MnO_2 coatings, Cr_2O_3 was mixed with MnO_2 powder, $MnCo_2O_4$ powder and the $MnCo_2O_4$–MnO_2 mixture, respectively. According to the Mn–Cr diagram in air [14], solid solutions of spinel phase appear at a temperature above 720 °C. To accelerate the solid-state reaction, the oxide mixtures were kept at 900 °C for 6 h, and the crystal structures of the products were then analyzed by XRD. As indicated in the XRD profiles shown in Fig. 5, Cr_2O_3 can react with MnO_2 and/or $MnCo_2O_4$ in all cases, which produces $(Mn,Cr)_3O_4$ and $(Mn,Co,Cr)_3O_4$ spinel solid solutions. This behavior may explain the appearance of an interfacial reaction layer simultaneously containing Mn, Co and Cr, as shown in Figs. 3 and 4. On the other hand, although Cr_2O_3 easily reacts with the coating materials, Cr migration in the spinel oxides is quite slow at 800 °C. In the region away from the interface, only a small amount of Cr can be noticed even after holding at 800 °C for 1000 h (Figs. 3 and 4).

As suggested in our previous study [20], the interface between a well-conducting coating and a metallic substrate dominates the

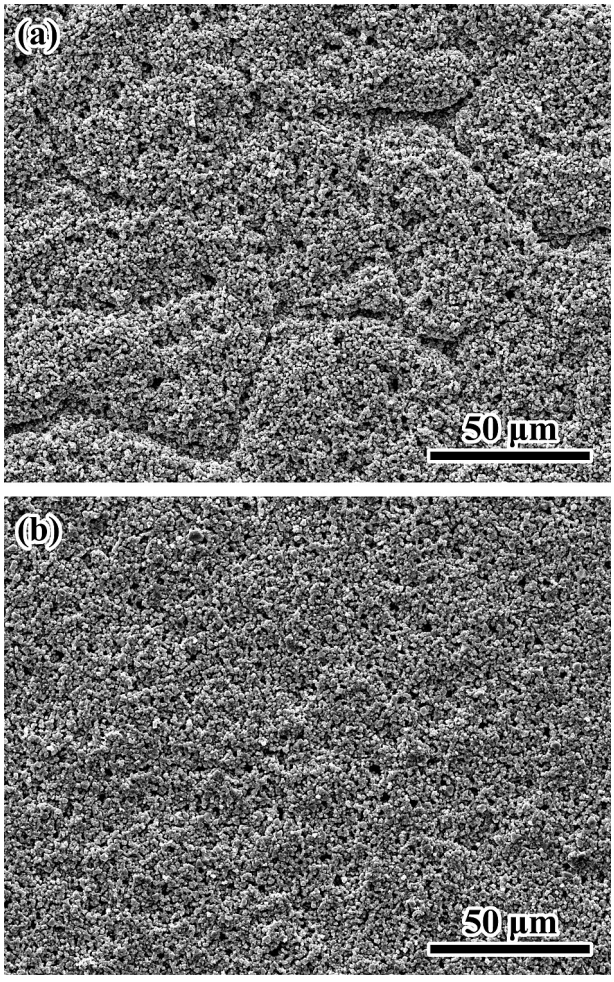

Fig. 2. SEM images of $MnCo_2O_4$–MnO_2-coated SUS430 plates after oxidation at 800 °C for 1000 h. The samples were pre-oxidized at 800 °C for (a) 2 h and (b) 25 h before slurry coating.

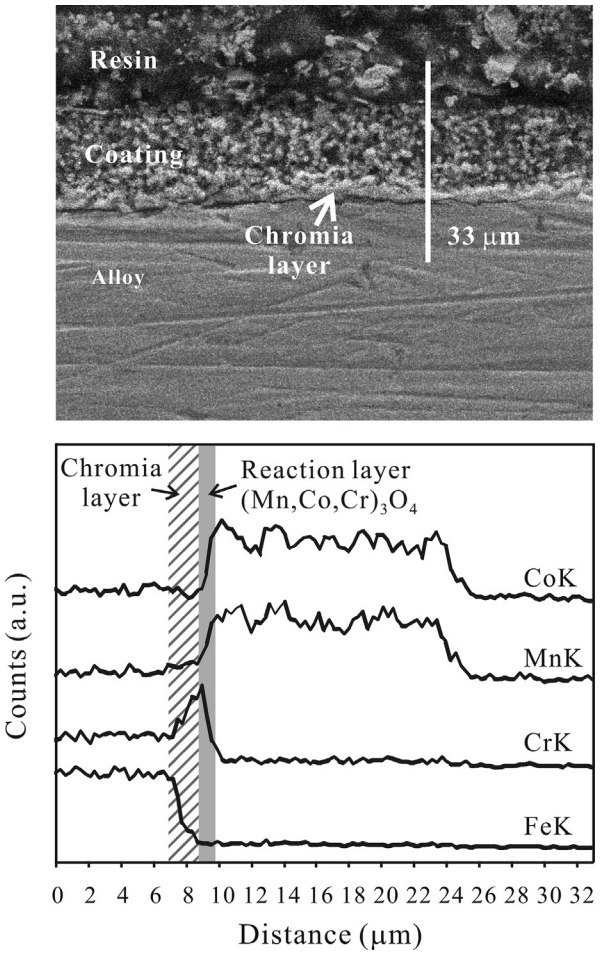

Fig. 3. Cross-sectional SEM image and the profile of EDX line-scan of $MnCo_2O_4$–MnO_2-coated SUS430 plates (pre-oxidized for 2 h) after oxidation at 800 °C for 1000 h.

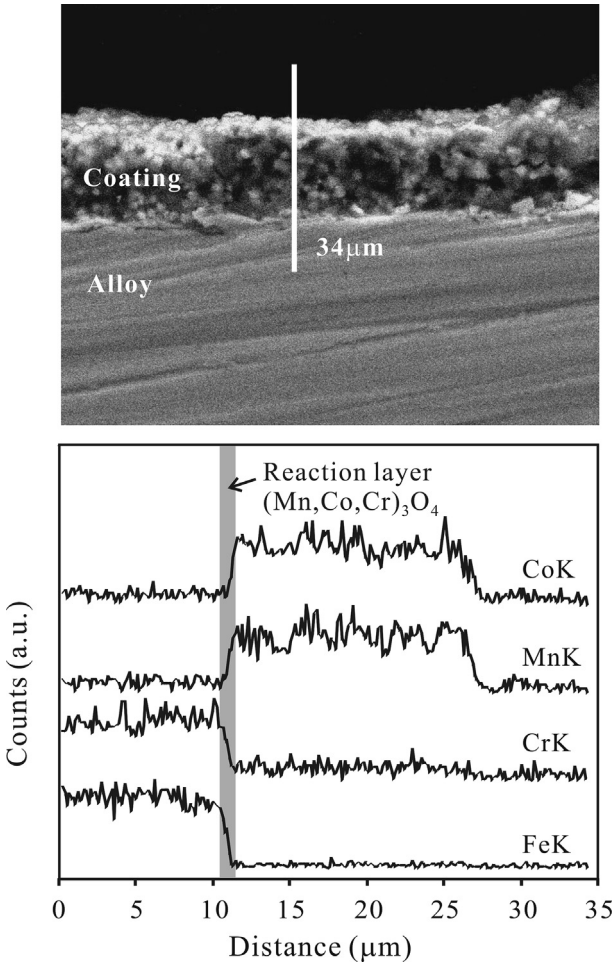

Fig. 4. Cross-sectional SEM image and the profile of EDX line-scan of $MnCo_2O_4$–MnO_2-coated SUS430 plates (pre-oxidized for 25 h) after oxidation at 800 °C for 1000 h.

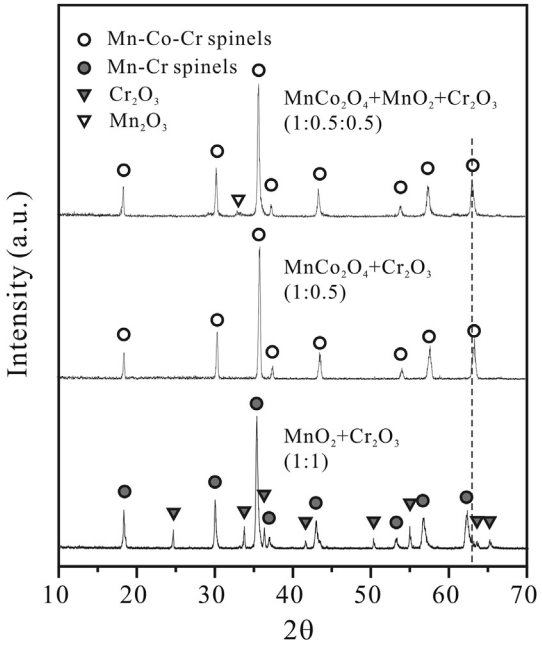

Fig. 5. XRD profiles of the mixed powders after heating at 900 °C for 6 h: (1) MnO_2 and Cr_2O_3, (2) $MnCo_2O_4$ and Cr_2O_3 and (3) $MnCo_2O_4$, MnO_2 and Cr_2O_3. The mole ratios of different components in the mixture are shown in the figure.

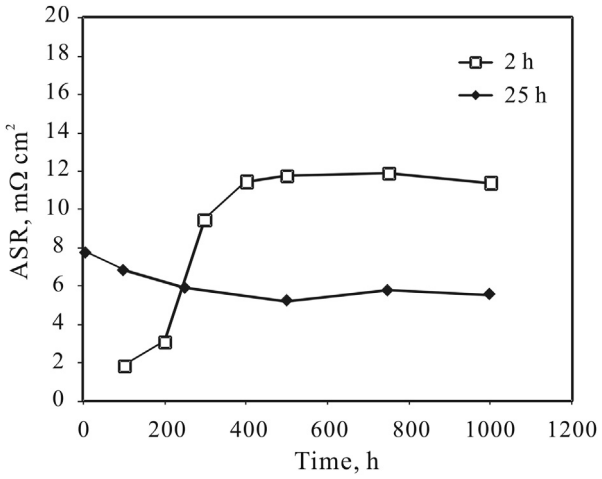

Fig. 6. ASR of the $MnCo_2O_4$–MnO_2-coated SUS430 plates pre-oxidized at 800 °C for 2 h and 25 h.

electrical properties of the coated metallic interconnects. In the present study, the interfacial region may include the reaction layer and the oxidation layer produced during coating preparation and the following oxidation tests. It is believed that the distinct interfacial microstructures caused by pre-oxidation treatment for various periods could lead to quite different electrical properties. Fig. 6 displays ASR curves of the coated SUS430 samples through 1000 h of oxidation at 800 °C. The ASR of the sample pre-oxidized for 25 h slightly decreased at the beginning, which could be due to the subtle increase in the density of the protective layer. Then, the ASR remained low (≈ 6 mΩ cm^2) until reaching 1000 h of testing. In contrast, the ASR of the sample pre-oxidized for 2 h rapidly increased from approximately 2 mΩ cm^2 to 12 mΩ cm^2 during the first 500 h, implying that the oxidation of the metallic substrate could take place even under the protection of a $MnCo_2O_4$–MnO_2 coating. However, after 500 h of oxidation, the ASR of the 2 h pre-oxidized samples remained at approximately 12 mΩ cm^2, which was twice that of the sample pre-oxidized for 25 h. Fig. 7 shows Arrhenius plots of the coated samples after 1000 h of oxidation

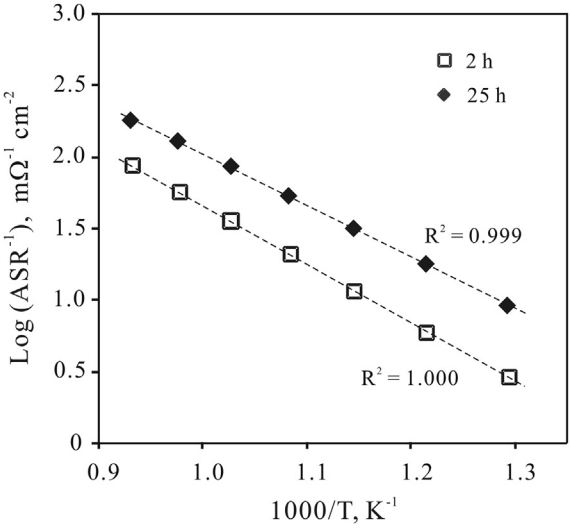

Fig. 7. Arrhenius plots of the $MnCo_2O_4$–MnO_2-coated SUS430 plates after 1000 h of oxidation tests at 800 °C. The linear correlation coefficients (R) of the data and the lines used to determine the activation energies are also presented in the figure.

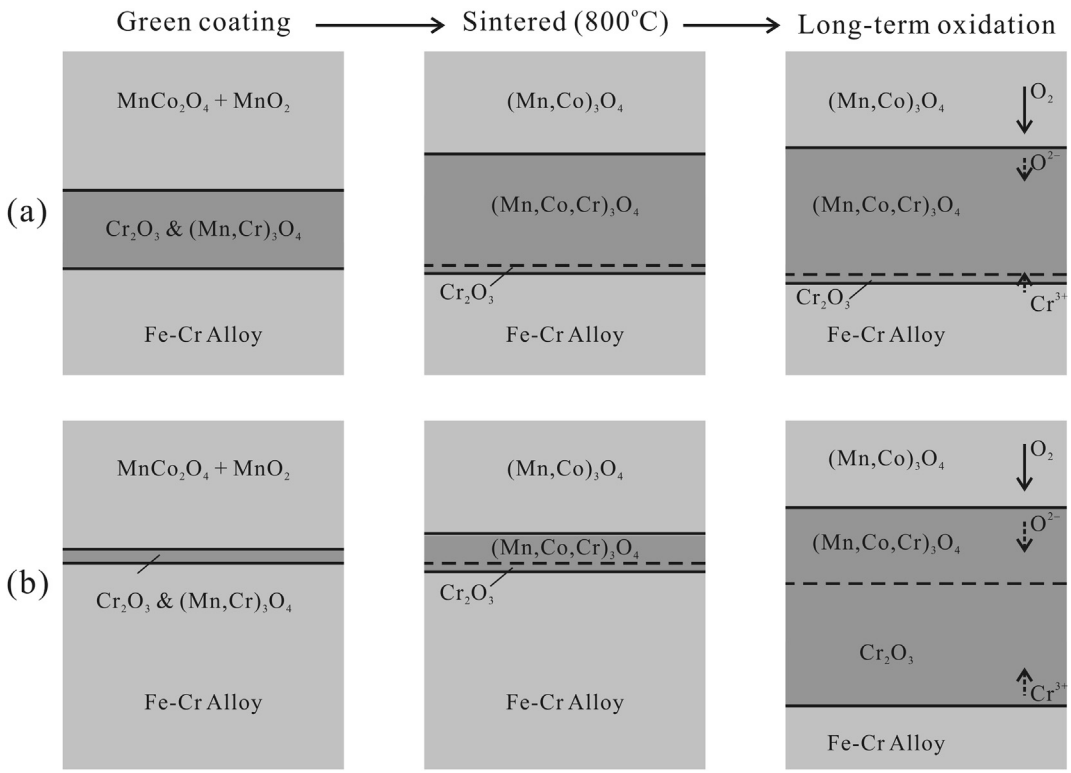

Fig. 8. A schematic of the formation of the reaction layer and its effect on the following oxidation tests with (a) a thicker pre-oxidized scale and (b) a thinner pre-oxidized scale.

tests. The activation energy for electrical conduction is 83 kJ mol^{-1} and 76 kJ mol^{-1} for the samples pre-oxidized for 2 h and 25 h, respectively. A comparison of the microstructural and compositional features shown in Figs. 3 and 4 indicates that the differences in ASR and activation energy are mainly due to the distinct interfacial structures of these samples.

By taking all of these results into account, we suspect that the dense $(Mn,Co,Cr)_3O_4$ layer produced by the solid-state reactions between the coating and the pre-oxidized alloy could be the key to hindering the diffusion of oxygen and improving the oxidation resistance of the coated alloy. Fig. 8 illustrates the formation of the reaction layer and its effect on the oxidation of the coated alloy. During the sintering process, a pre-oxidized scale with a suitable thickness (e.g., ≈0.5 μm on the sample pre-oxidized for 25 h) could promote the formation of a thicker $(Mn,Co,Cr)_3O_4$ reaction layer. Although oxygen could reach the coating-alloy interface through the pores in the low-temperature-sintered coating, the dense reaction layer can suppress the further migration of oxygen during oxidation tests (Fig. 8(a)). On the other hand, the diffusion of Cr in Mn–Co or Mn–Cr spinel oxides is much slower than that in Cr_2O_3. Therefore, a thicker reaction layer can effectively restrain the oxidation beneath the coating. In contrast, if the $(Mn,Co,Cr)_3O_4$ reaction layer is thin or discontinuous, oxygen and/or chromium could penetrate through this thin layer (Fig. 8(b)). In this case, the alloy will be considerably oxidized until a dense reaction layer with sufficient thickness forms during long-term oxidation. In the present study, the profiles of EDX line-scans (Figs. 3 and 4) revealed that the "sufficient thickness" of an effective reaction layer could be approximately 1 μm. Further increasing the thickness of the reaction layer by extending the pre-oxidation period may enhance the oxidation resistance. However, it reduces the electrical properties of the coated alloy because the conductivity of $(Mn,Co,Cr)_3O_4$ is lower than that of the coating materials. As shown in Fig. 9, although the ASR of the sample pre-oxidized for 100 h also decreases during long-term oxidation, its ASR value is always higher than that of the sample pre-oxidized for 25 h. This result suggests that an optimized pre-oxidation treatment is important to achieving spinel-coated SUS430 with excellent oxidation resistance and high electrical performance. For the materials examined in this work, 25 h of pre-oxidation at 800 °C is optimum in terms of both oxidation resistance and electrical properties.

Lastly, Table 1 compares the characteristics of the coatings studied in this work with those formed by a reduction treatment. The results show that all of techniques can produce effective protective coatings with low ASR values. Because the cost and risk associated with heat treatment in hydrogen are much higher than

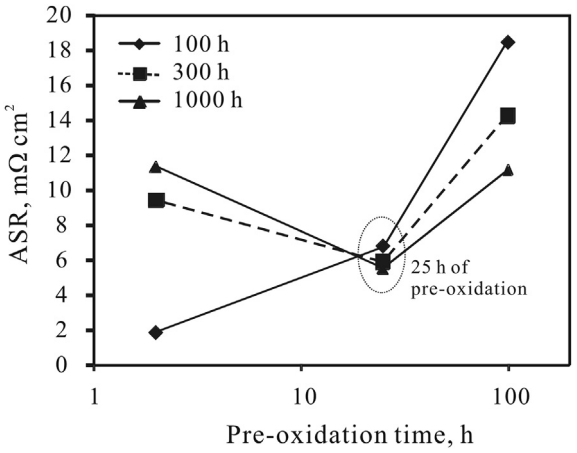

Fig. 9. ASR of the $MnCo_2O_4$–MnO_2-coated SUS430 plates after 100 h, 200 h and 1000 h of oxidation tests at 800 °C.

Table 1
A comparison of the spinel coatings prepared by different techniques. All samples were oxidized at 800 °C for 1000 h before microstructural characterization and ASR measurement.

Technique	Pre-treatment	Air sintering	Morphology	Coating alloy interface		ASR, mΩ cm^2	Refs.
				Reaction layer[a]	Chromia scale		
Multi-component coating	Pre-oxidation at 800 °C for 25 h	800 °C	Porous	~1 μm	negligible	~6	This study
With a reduction of green coatings	Reduction at 800 °C for 20–24 h	800–850 °C	Porous	~1–1.5 μm	~1.5–2 μm	~7–15[b]	[13,16,17]
With a reduction of nanopowders	Reduction at 700 °C for 2 h	800–900 °C	With nanopores	~1.5 μm	~1 μm	~3–4	[18,19]

[a] Roughly estimated from the EDX line-scan profiles published in the references.
[b] ASR measured with a perovskite contact layer.

those associated with heat treatment in air, the coating technique presented in this study could be less expensive and safer than those required a reduction stage. On the other hand, as shown in Table 1, an interfacial reaction layer with a thickness of approximately 1–1.5 μm may also be observed in the samples prepared by a reduction treatment [13,16–19]. We believe that in those cases, the interfacial layer is also important to the oxidation resistance of the coated alloys because to date it is still difficult to obtain fully dense coatings through the low-temperature sintering techniques compared in Table 1.

4. Conclusions

Pre-oxidation treatment before slurry coating is critically important to improving the oxidation resistance of metallic interconnects coated with a low-temperature-sintered spinel layer. Microstructural and electrical characterizations show that a longer period of pre-oxidation at 800 °C could improve the oxidation resistance of spinel-coated SUS430. In terms of both oxidation resistance and electrical properties, 25 h of pre-oxidation at 800 °C is optimum for the materials examined in this work. Furthermore, it was revealed that the effect of pre-oxidation on the oxidation resistance and electrical properties may be due to its effect on the interfacial reactions between the coating and the pre-oxidized alloy. It is therefore suggested that the control and optimization of the coating-alloy interface could be the key to developing novel coating materials and technologies for SOFC metallic interconnects.

Acknowledgment

The financial supports of the National Natural Science Foundation of China (No. 51101146), the National Basic Research Program of China (No. 2012CB215500 and 2010CB732302), the National High Technology Research and Development program of China (Grant No. 2011AA050704) and the Scientific Research Foundation for the Returned Overseas Chinese Scholars, State Education Ministry are gratefully acknowledged.

References

[1] N. Shaigan, W. Qu, D.G. Ivey, W. Chen, J. Power Sources 195 (2010) 1529–1542.
[2] Z. Yang, Int. Mater. Rev. 53 (2008) 39–54.
[3] J.W. Fergus, Mater. Sci. Eng. A 397 (2005) 271–283.
[4] B. Hua, J. Pu, F. Lu, J. Zhang, B. Chi, L. Jian, J. Power Sources 195 (2010) 2782–2788.
[5] T. Horita, Y. Xiong, H. Kishimoto, K. Yamaji, N. Sakai, H. Yokokawa, J. Power Sources 131 (2004) 293–298.
[6] H. Kurokawa, K. kawamura, T. Maruyama, Solid State Ionics 168 (2004) 13–21.
[7] I. Antepara, I. Villarreal, L.M. Rodríguez-Martínez, N. Lecanda, U. Castro, A. Laresgoiti, J. Power Sources 151 (2005) 103–107.
[8] J. Froitzheim, G.H. Meier, L. Niewolak, P.J. Ennis, H. Hatterndorf, L. Singheiser, W.J. Quadakkers, J. Power Sources 178 (2008) 163–173.
[9] T. Uehara, N. Yasuda, M. Okamoto, Y. Baba, J. Power Sources 196 (2011) 7251–7256.
[10] Z. Yang, G.-G. Xia, C.-M. Wang, Z. Nie, J. Templeton, J.W. Stevenson, P. Singh, J. Power Sources 183 (2008) 660–667.
[11] Z. Yang, G.-G. Xia, X.-H. Li, J.W. Stevenson, Int. J. Hydrogen Energy 32 (2007) 3648–3654.
[12] B. Hua, J. Pu, W. Gong, J. Zhang, F. Lu, L. Jian, J. Power Sources 185 (2008) 419–422.
[13] Z. Yang, G. Xia, Z. Nie, J. Templeton, J.W. Stevenson, Electrochem. Solid State Lett. 11 (2008) B140–B143.
[14] A. Petric, H. Ling, J. Am. Ceram. Soc. 90 (2007) 1515–1520.
[15] W. Qu, L. Jian, J.M. Hill, D.G. Ivey, J. Power Sources 153 (2006) 114–124.
[16] Z. Yang, G. Xia, Z. Nie, J. Templeton, J.W. Stevenson, Electrochem. Solid State Lett. 11 (2005) A168–A170.
[17] Patent: Y. Baba, H. Kameda, H. Kurokawa, Y. Matsuzaki, K. Ogasawara, S. Yamashita, Protection film coating method on interconnector for SOFC, TOKYO GAS CO LTD, JP2009-152016A.
[18] X. Xin, S. Wang, Q. Zhu, Y. Xu, T. Wen, Electrochem. Commun. 12 (2010) 40–43.
[19] X. Xin, S. Wang, J. Qian, C. Lin, Z. Zhan, T. Wen, Int. J. Hydrogen Energy 37 (2012) 471–476.
[20] D.R. Ou, M. Cheng, X.-L. Wang, J. Power Sources 236 (2013) 200–236.
[21] JCPDS – International Center for Diffraction Data, Card No. 33-0892 ($Mn_{1.5}Cr_{1.5}O_4$), Card No. 75-1614 ($MnCr_2O_4$), Card No. 23-1237 ($MnCo_2O_4$), Card No. 24-0507 (Mn_2O_3), Card No. 38-1479 (Cr_2O_3).